Heliyon 10 (2024) e25460

Contents lists available at ScienceDirect

Heliyon

journal homepage: www.cell.com/heliyon

Research article

Human umbilical cord mesenchymal stem cells attenuate diet-induced obesity and NASH-related fibrosis in mice

Jiali Hu [a,1], Shan Li [a,1], Xuan Zhong [a], Yushuang Wei [b], Qinjuan Sun [a], Lan Zhong [a,b,*]

[a] Department of Gastroenterology, Shanghai East Hospital, Tongji University School of Medicine, Shanghai, China
[b] Shanghai Institute of Stem Cell Research and Clinical Translation, Shanghai, 200120, China

ARTICLE INFO

Keywords:
Mesenchymal stem cell
Non-alcoholic steatohepatitis
Fatty liver
Fibrosis

ABSTRACT

Non-alcoholic steatohepatitis (NASH) is a progressive form of non-alcoholic fatty liver disease (NAFLD) that may progress to cirrhosis and hepatocellular carcinoma but has no available treatment. Mesenchymal stem cells (MSCs) have become increasingly prominent in cell therapy. Human umbilical cord MSCs (hUC-MSCs) are considered superior to other MSCs due to their strong immunomodulatory ability, ease of collection, low immune rejection, and no tumorigenicity. Though hUC-MSCs have received increasing attention in research, they have been rarely applied in any investigations or treatments of NASH and associated fibrosis. Therefore, this study evaluated the therapeutic efficacy of hUC-MSCs in C57BL/6 mice with diet-induced NASH. At week 32, mice were randomized into two groups: phosphate-buffered saline and MSCs, which were injected into the tail vein. At week 40, glucose metabolism was evaluated using glucose and insulin tolerance tests. NASH-related indicators were examined using various biological methods. hUC-MSC administration alleviated obesity, glucose metabolism, hepatic steatosis, inflammation, and fibrosis. Liver RNA-seq showed that the expression of the acyl-CoA thioesterase (ACOT) family members Acot1, Acot2, and Acot3 involved in fatty acid metabolism were altered. The cytochrome P450 (CYP) members Cyp4a10 and Cyp4a14, which are involved in the peroxisome proliferator-activator receptor (PPAR) signaling pathway, were significantly downregulated after hUC-MSC treatment. In conclusion, hUC-MSCs effectively reduced Western diet-induced obesity, NASH, and fibrosis in mice, partly by regulating lipid metabolism and the PPAR signaling pathway.

1. Introduction

Obesity is one of the most prevalent health issues globally. It is associated with metabolic comorbidities, including non-alcoholic fatty liver disease (NAFLD), and clinicopathological syndromes characterized by excessive intracellular fat deposition in the liver. NAFLD, which has a worldwide incidence of approximately 25 %, comprises subtypes, including simple fatty liver, non-alcoholic steatohepatitis (NASH), and cirrhosis [1–4]. The natural history of NASH is changeable; however, approximately 30 % of patients progress to cirrhosis and hepatocellular carcinoma [5]. Furthermore, NASH is associated with an increased risk of extra-liver disorders,

* Corresponding author. Department of Gastroenterology, Shanghai East Hospital, Tongji University School of Medicine, Shanghai, China. Shanghai Institute of Stem Cell Research and Clinical Translation, Shanghai, China.
E-mail address: lanzhong@tongji.edu.cn (L. Zhong).
[1] These authors contributed equally to this work.

https://doi.org/10.1016/j.heliyon.2024.e25460
Received 12 September 2023; Received in revised form 26 January 2024; Accepted 26 January 2024
Available online 1 February 2024

Abbreviations

ACOT	acyl-CoA thioesterase
ALT	alanine aminotransferase
AST	aspartate aminotransferase
BM	bone marrow-derived
COL	collagen
CYP	cytochrome P450
CPT1A	carnitine palmitoyltransferase 1A
DEGs	Differentially expressed genes
FC	fold change
FPKM	fragments per kilobase of transcript per million mapped reads
GEO	gene expression omnibus
GTT	glucose tolerance test
GO	gene ontology
HFD	high-fat diet
hUC	human umbilical cord
H&E	hematoxylin and eosin
ITT	insulin tolerance text
KEGG	Kyoto encyclopedia of genes and genomes
MCD	methionine-choline-deficient diet
MSC	mesenchymal stem cell
NAFLD	non-alcoholic fatty liver disease
NASH	non-alcoholic steatohepatitis
PBS	phosphate-buffered saline
PPAR	peroxisome proliferator-activator receptor
qPCR	Quantitative Polymerase Chain Reaction
RNA-seq	RNA sequencing
TNF-α	Tumor necrosis factor-alpha
VAT	visceral adipose tissue
WD	western diet
α-SMA	Actin alpha

including obesity, cardiovascular diseases, diabetes, colon cancer, and their related mortality [6]. As the most critical form of NAFLD, hepatic fibrosis is the most important determinant of mortality in patients with NASH. Treating NASH and NASH-related fibrosis can improve the prognosis of adverse hepatic consequences and non-liver-associated outcomes [7]. Unfortunately, there is currently no approved pharmacotherapy for NASH or fibrosis. The most effective treatment for NASH is diet and weight loss, which have proven difficult to achieve and sustain. Consequently, NASH and advanced fibrosis patients have unmet medical needs [8].

Mesenchymal stem cell (MSC) therapy has become a hot topic in research owing to its regenerative, immunomodulatory, and anti-inflammatory functions [9]. MSCs have been used to treat acute tissue injury syndromes, chronic degenerative disorders, cardiovascular diseases [10], graft-versus-host disease [11], and inflammatory disorders [12], such as Crohn's disease [13]. MSCs have three main types: human bone marrow-derived MSCs (BM-MSCs), human adipose-derived MSCs, and human umbilical cord stem cells (hUC-MSCs). Human BM-MSCs are generally obtained from bone marrow discarded from knee or hip surgery. Hence, these stem cells' proliferative and differentiation capacities are significantly reduced, and their transplantation into allogeneic bodies may result in immune reactions, thereby limiting their clinical applications. MSCs can also be extracted from various vascularized tissues, such as hUC-MSCs, which are abundant in perinatal tissues [14]. hUC-MSCs possess significant regenerative and therapeutic potentials; their added benefits include their ease of collection, an endless source of stem cells, reduced immune rejections, no tumorigenicity, and no ethical controversies. Considering that hUC-MSCs are more suitable for clinical applications, we selected hUC-MSCs for our study to observe their effects on NASH and fibrosis. To our knowledge, no study has investigated the application of hUC-MSCs in treating Western diet (WD)-induced NASH in mice. More importantly, whether this therapy can reduce obesity and NASH-related fibrosis requires further investigation. Thus, the present study aimed to determine whether hUC-MSCs could alleviate WD-induced obesity, steatosis, inflammation, and fibrosis, which may provide an experimental basis for the future treatment of obesity-related NASH.

2. Materials and methods

2.1. Isolation and identification of MSCs from the human umbilical cord

The hUC-MSCs used in our research were derived from the National Stem Cell Transformation Resource Bank and were successfully produced on a large scale. All hUC-MSCs passed the quality review inspection of China's Food and Drug Administration (report

number: SH201903852/SH201903853) and met the requirements for clinical use. The Institutional Review Board of Shanghai East Hospital authorized our human umbilical cord collection, and human umbilical cords were collected from the Maternity Department of Shanghai East Hospital with the patient's permission. Methods for the isolation and processing of hUC-MSCs had been previously described in detail [15]. Flow cytometry analysis (BD Biosciences) was performed on the fifth passage of hUC-MSCs after 30 min of incubation with phycoerythrin- or fluorescein isothiocyanate-conjugated mouse monoclonal antibodies against human CD11, CD19, CD31, CD34, CD45, HLA-DR, CD73, CD90, and CD105 (1:50). Differentiation was identified by replacing the culture medium with complete osteogenic, adipogenic, or chondrocyte differentiation media (A10066, A10069, and A10064; Thermo Fisher Scientific) to induce osteogenesis, adipogenesis, and chondrogenesis, respectively. Cells were stained with Alizarin Red S, Alcian Blue, or Oil Red O after stimulation. The fifth passage of hUC-MSCs was used to treat NASH mice. The antibodies used are listed in Table S1.

2.2. Animals and treatments

Five-week-old male C57BL/6J mice (18–20 g) were purchased from GemPharma Tech and housed in an animal facility at Shanghai East Hospital. All animal experiments were conducted in accordance with the University of Health Guide for the Care and Use of Laboratory Animals and were authorized by the Biological Research Ethics Committee of Tongji University. Ten mice were fed a WD (fat, 40 %; fructose, 20 %; cholesterol, 2 %; trophic). At 32 weeks after the start of feeding, the mice were randomized into the NASH-phosphate-buffered saline (PBS) group (n = 5) or NASH-MSC group (n = 5) and were injected with PBS as the solute control or hUC-MSCs (1.5×10^6 cells), respectively, once into the tail vein. WD was continued for another 8 weeks, the mice were euthanized, and their liver, serum, and visceral adipose tissue (VAT) were obtained.

2.3. Histological analysis

The liver and VAT were fixed in 4 % paraformaldehyde, embedded in paraffin, or frozen following standard procedures. Paraffin-embedded liver sections were used for hematoxylin and eosin (H&E) and Sirius red staining, and OCT-embedded liver sections were used for Oil Red O staining.

2.4. Glucose tolerance test (GTT) and insulin tolerance test (ITT)

Glucose metabolism was detected using the GTT and ITT. For the GTT, the mice were fasted for 18 h and then 1.2 g/kg of glucose was administered via intraperitoneal injection; ITT was performed via intraperitoneal injection with 0.7 U/kg of recombinant human insulin (Novo Nordisk A/S) after 6-h fasting. Blood glucose was determined at 0, 15, 30, 60, 90, and 120 min using an Accu-Chek glucometer (Roche) after glucose/insulin administration.

2.5. Western blot analysis

Liver tissues were lysed in RIPA lysis buffer (50 mM Tris-HCl pH 7.4, 150 mM NaCl, 1 % Triton X-100, 1 % sodium deoxycholate, 0.1 % SDS) supplemented with PMSF and a protease inhibitor (Roche). Liver tissue lysates were then subjected to SDS-PAGE, transferred to polyvinylidene difluoride (PVDF) membranes, and blotted with antibodies. Membranes were blocked in TBS with 1 % Tween-20 and 5 % milk for 1 h and incubated with primary antibodies overnight at 4 °C. Goat anti-mouse IgG (Thermo, 31460) or goat anti-rabbit IgG (Thermo, 31430) were used as secondary antibodies. Restore™ Western Blot Stripping Buffer was used to cover the blot for incubation of 5–15 min at 37 °C with gentle shaking to remove primary and secondary antibodies from the western blots. The primary antibodies used are listed in Table S1.

2.6. Quantitative polymerase chain reaction (qPCR) analysis

Total RNA was extracted by RNAeasy kit (R0027; Beyotime) following the manufacturer's instructions. We reverse-transcribed 1 μg of total RNA from all samples using the PrimeScript™ RT reagent Kit with gDNA Eraser (RR047A; TaKaRa). qPCR analysis was performed using TB Green Premix Ex Taq (RR420A; TaKaRa) with the Applied Biosystems 7500 Fast Real-Time PCR System (Thermo Fisher Scientific). The primers are listed in Table S2.

2.7. Biochemical assays

Alanine aminotransferase (ALT) and aspartate aminotransferase (AST) levels were measured using the Chemray 800 automatic analyzer (Rayto Life and Analytical Sciences Co).

2.8. RNA sequencing (RNA-seq) and bioinformatics analysis

A cDNA library was constructed from two different treated WD-induced groups (n = 3, separately), and their livers' total RNA was sequenced with Illumina Novaseq™ 6000 sequence platform. Using the Illumina paired-end RNA-seq approach, we sequenced the transcriptome, generating 2 × 150 bp paired-end reads. To obtain high-quality clean reads, these reads were further filtered by Cutadapt [16]. The sequence quality was verified using FastQC (http://www.bioinformatics.babraham.ac.uk/projects/fastqc/, 0.11.9). A total of 35.3 Gbp of cleaned, paired-end reads were produced. The filtered reads were mapped to the mouse reference genome GRCm38/mm10 using Hisat2 (v2.2.1) [17]. The mapped reads were assembled using Stringtie (v2.1.6) [18], and transcripts

were merged using Gffcompare (v0.9.8) [19]. The expression levels of these transcripts were estimated with the Fragments Per Kilobase of transcript per Million mapped reads method using Stringtie (v2.1.6) and Ballgown (v2.30.0) [20]. Differentially expressed genes (DEGs) were then identified using DESeq2 (v1.28.1). The threshold for up-and down-regulated genes was $P \leq 0.05$ and an absolute fold change (FC) ≥ 2.0. The DEGs were used for the downstream enrichment analysis of Gene Ontology (GO) functions and Kyoto Encyclopedia of Genes and Genomes (KEGG) pathways. The raw sequence data and processed data have been submitted to the

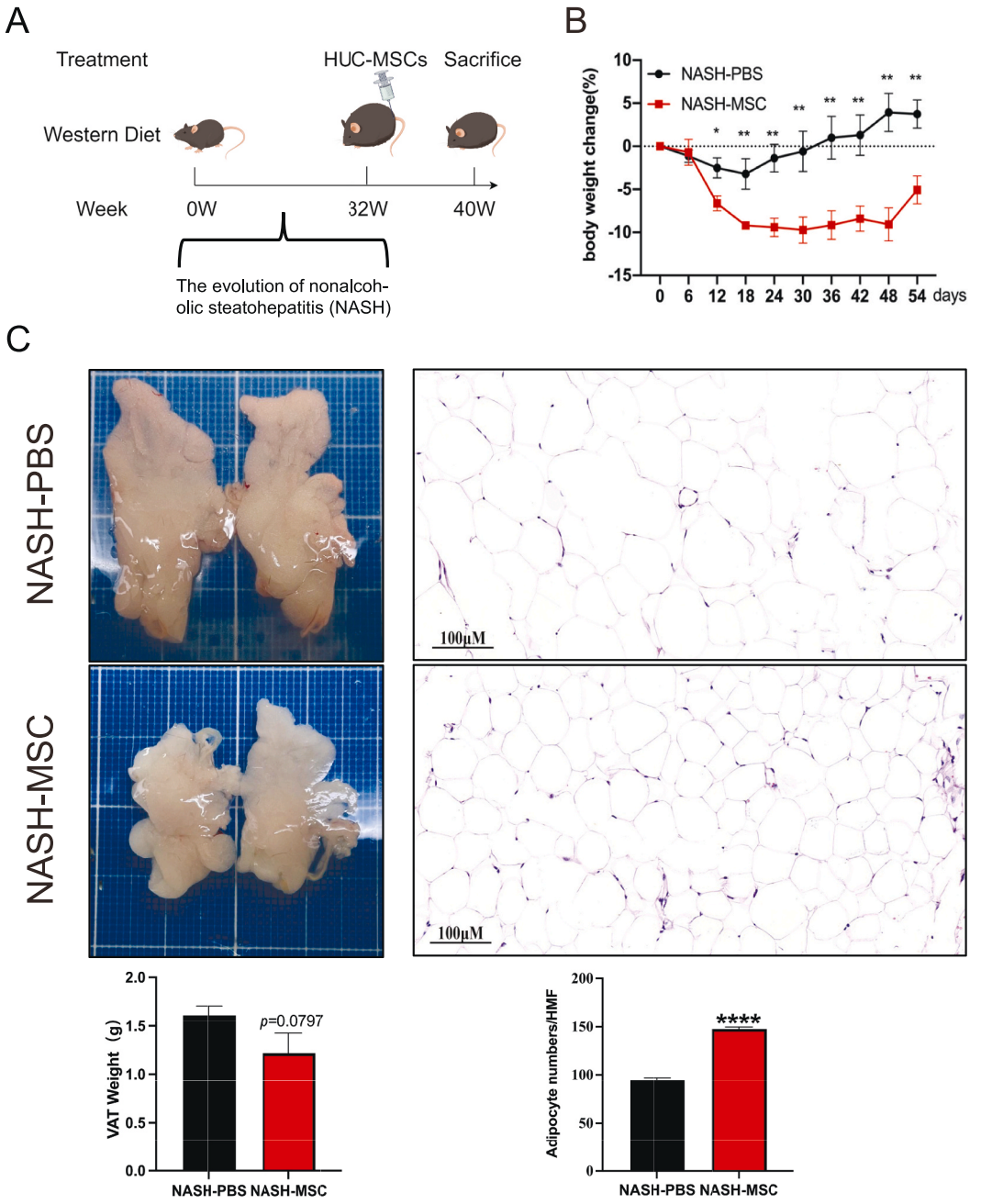

Fig. 1. hUC-MSCs administration alleviated WD-induced obesity in mice (A) Experimental flow chart. 5-week-old C57BL/6j male mice were given WD (containing 40 % fat, 20 % fructose, 2 % cholesterol) for 32 weeks and then divided into 2 groups with a single tail vein injection of PBS 200 μL or hUC-MSCs 1.5 × 10^6 cells/only and continued WD feeding for 8 weeks before execution. (by Figdraw) (B) Body weights of mice at different time points after tail vein injection of drugs (after week 32). (C) Appearance and weight of representative VAT of both groups (above, NASH-PBS; below, NASH-MSC). (D) HE staining (original magnification, × 200) and adipocyte number/HMF of representative VAT of both groups. HMF: High magnification field. The data are presented as the means ± SEM. NASH-PBS ($n = 4$) and NASH-MSC ($n = 5$), respectively, $^{*}p < 0.05$, $^{**}p < 0.01$, $^{****}p < 0.0001$.

NCBI Gene Expression Omnibus (GEO) datasets with accession number <GSE224233>.

2.9. Statistical analysis

All experiments were performed at least three times, and the results were reported as the mean ± standard error of the mean (SEM). GraphPad Prism 7.0 software (GraphPad Software, La Jolla, CA, USA) was used to evaluate statistical significance. After testing for normal distribution using the Shapiro–Wilk normality test, significant differences between samples were calculated using the unpaired Student's t-test or the Mann–Whitney U-rank test. $p < 0.05$ was considered statistically significant.

3. Results

3.1. hUC-MSCs administration alleviated WD-induced obesity in mice

hUC-MSCs were identified using flow cytometry, as previously reported [21,22]; more than 95 % were positive for CD73/CD90/CD105, whereas fewer than 1 % were positive for CD11/CD19/CD31 and CD34/CD45/HLA-DR (Fig. S1A). Furthermore, hUC-MSCs successfully differentiated into adipocytes, osteoblasts, and chondrocytes in vitro (Fig. S1B); these were the identification marks of MSCs.

The flowchart of experiments is shown in Fig. 1A. From 12 days after hUC-MSCs injection until the end of the experiment, the body weight of the MSC-treated group was remarkably lower than that of the PBS-control group (Fig. 1B). No notable differences in VAT weight were noted between MSC-treated and PBS-control WD mice (Fig. 1C); however, the number of adipocytes visualized by H&E staining was considerably greater in MSC-treated mice than in PBS-control mice (Fig. 1D), indicating that the application of hUC-MSCs reduced the size of adipocytes.

3.2. hUC-MSC Application Modulated Glucose Metabolism

GTT (Fig. 2A) and ITT (Fig. 2B) assays revealed that hUC-MSC application markedly improved glucose tolerance and insulin

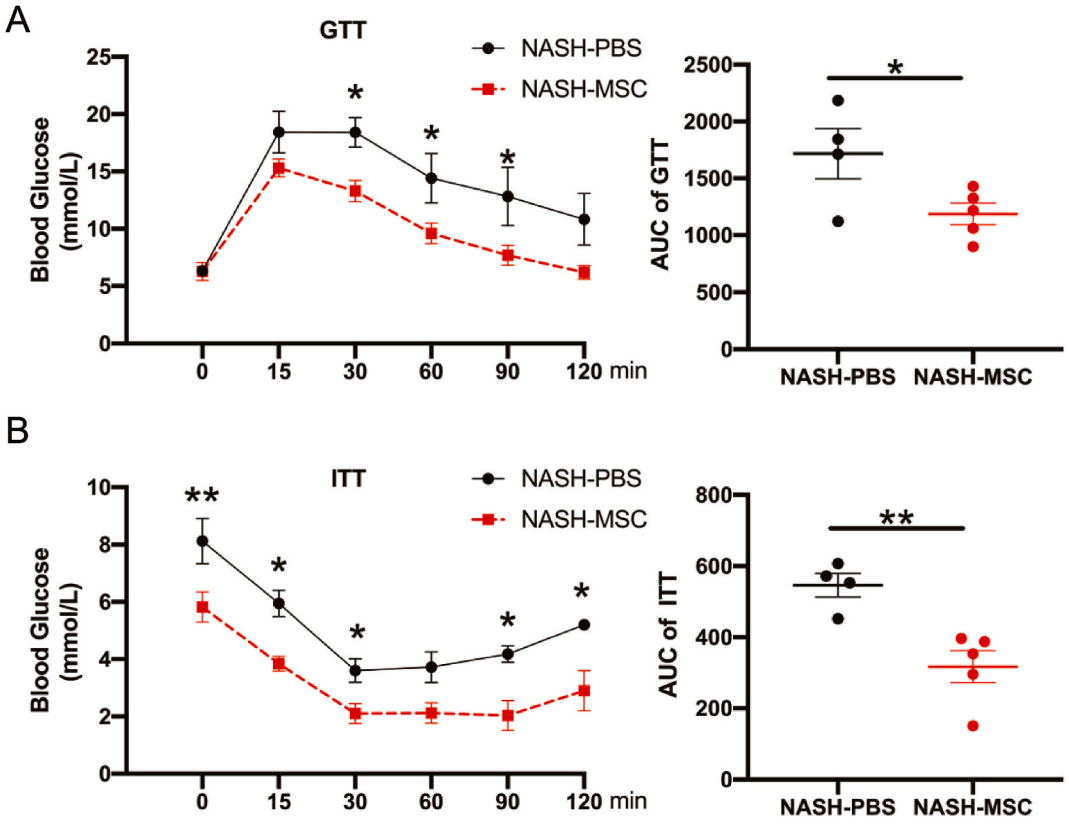

Fig. 2. hUC-MSCs application modulated glucose metabolism (A) Blood glucose levels and the area under the curve for glucose during GTT (NASH-PBS $n = 4$ and NASH-MSC $n = 5$, respectively). (B) Blood glucose levels and the area under the curve for glucose during ITT (NASH-PBS $n = 4$ and NASH-MSC $n = 5$, respectively). The data are expressed as the means ± SEM. *$p < 0.05$, **$p < 0.01$.

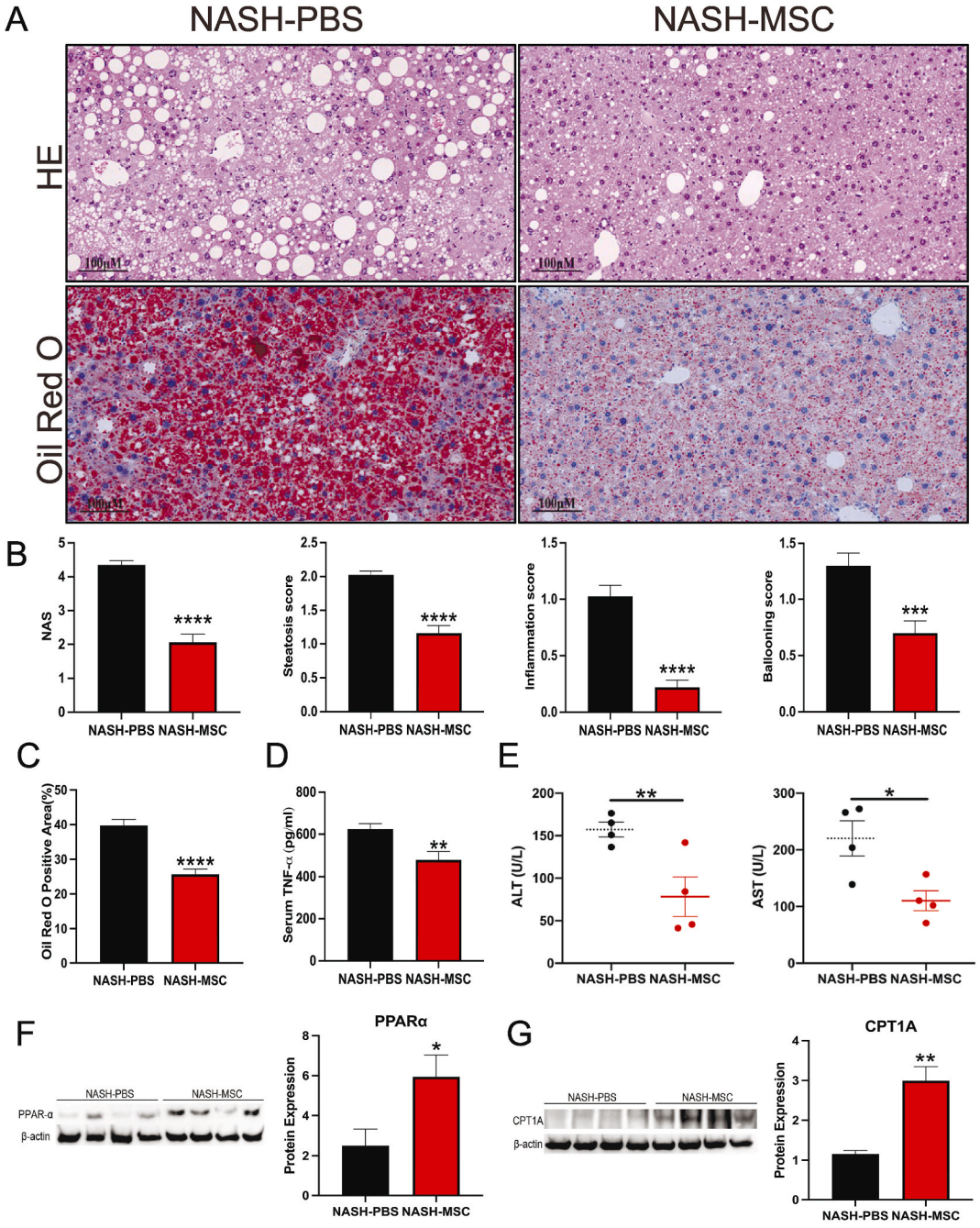

Fig. 3. hUC-MSCs transplantation alleviated hepatic steatosis and inflammation (A) HE and Oil Red O staining of liver sections from two groups of mice. (Scale bars, 100 μm) (B) NAFLD activity score (NAS) and Histological scoring of steatosis, hepatocyte ballooning, and lobular inflammation from both groups of mice (n = 4–5 mice/group). (C) Quantification of oil red O staining of liver sections from two groups of mice (n = 4–5 mice/group) (lower part of Fig. 3A). Positive areas were quantified with Image J. (D) TNF-α expression in the serum of both groups of mice determined by ELISA (n = 4–5 mice/group) (E) ALT and AST expression in the serum of both groups of mice (n = 4–5 mice/group). (F) PPARα protein expression in livers of indicated groups. (n = 4 mice/group). (the uncropped versions of the figures can be found in the supplement file). (G) CPT1A protein expression in livers of indicated groups. (n = 4 mice/group). (the uncropped versions of the figures can be found in the supplement file).

sensitivity. Collectively, these data suggest that the hUC-MSCs application improved insulin sensitivity and reversed the impaired glucose tolerance under a WD challenge.

3.3. hUC-MSC transplantation alleviated hepatic steatosis and inflammation

Hepatic steatosis and inflammation are strongly linked to obesity and insulin resistance. Hence, histological comparisons were performed between the livers of both groups. The livers of PBS-control mice were paler, bigger, and heavier than those of MSC-treated mice (Fig. S2). Fewer lipid droplets accumulated in the livers of MSC-treated mice, as visualized by Oil Red O and H&E staining (Fig. 3A). Additionally, hUC-MSC treatment significantly ameliorated these NASH phenotypes, as confirmed by quantitative histological analyses performed according to the extent of steatosis, lobular inflammation, and hepatocyte ballooning.

Furthermore, the NAFLD activity score was significantly lower in MSC-treated mice (Fig. 3B and C). In parallel with these morphological changes, serum AST and ALT levels were significantly diminished in the fifth week following hUC-MSC transplantation (Fig. 3E). Correspondingly, serum tumor necrosis factor-alpha (TNF-α) concentration immensely decreased in MSC-treated mice (Fig. 3D). Moreover, PPAR-α is a key transcriptional regulator of fatty acid oxidation in mitochondria. CPT1A, the liver isoform that catalyzes the rate-limiting step of converting acyl-coenzyme into acyl-carnitines, which can then cross membranes to get into the mitochondria. Both of them are considered a crucial metabolic regulator of hepatic lipid metabolism and inflammation. We further examined the expression of PPAR-α (Fig. 3F) and CPT1A (Fig. 3G) by Western Blotting and found the expressions of both significantly increased after hUC-MSCs treatment. These indicate that hUC-MSC treatment alleviates WD-induced hepatic steatosis and inflammation.

3.4. hUC-MSC treatment significantly attenuated NASH-related fibrosis in mice

Quantitative image analysis of Sirius red-stained liver slices showed less liver fibrosis in MSC-treated mice (Fig. 4A). Moreover, western blotting and qPCR confirmed the effect of hUC-MSCs in alleviating NASH-associated fibrosis. The expression of α-SMA protein was significantly decreased in the livers of MSC-treated mice, as compared with that in PBS control mice (Fig. 4B). Additionally, the mRNA expression levels of fibrosis-related collagen (COL) genes (*Col1a1*, *Col1a2*, and *Col3a1*) were downregulated in the livers of MSC-treated mice (Fig. 4C). These results indicate that hUC-MSC treatment attenuates fibrosis in NASH model mice.

3.5. hUC-MSC Administration Relieved NASH by Inhibiting the ACOT Gene Cluster and Cyp4a Family Members (Cyp4a10/Cyp4a14)

We performed RNA-seq analysis of liver samples from three mice per group to gain mechanistic insights into the amelioration of NASH by hUC-MSC treatment. Comparing livers from PBS control mice, we identified a total of 61 DEGs in the livers of MSC-treated mice, including 19 upregulated genes and 42 downregulated genes (Fig. 5A–C). The combination of GO-enriched biological process and KEGG-enriched top signaling pathway analyses led us to focus on fatty acid metabolic progress and the peroxisome proliferator-activator receptor (PPAR) signaling pathway (Fig. 5D–E). Volcano plots were generated to indicate the significantly altered metabolites and genes, which included the acyl-CoA thioesterase (ACOT) family members *Acot1*, *Acot2*, and *Acot3* (genes of fatty acid metabolic progress) and the cytochrome P450 (CYP) members *Cyp4a10* and *Cyp4a14* (genes of the PPAR signaling pathway) (Fig. 5B).

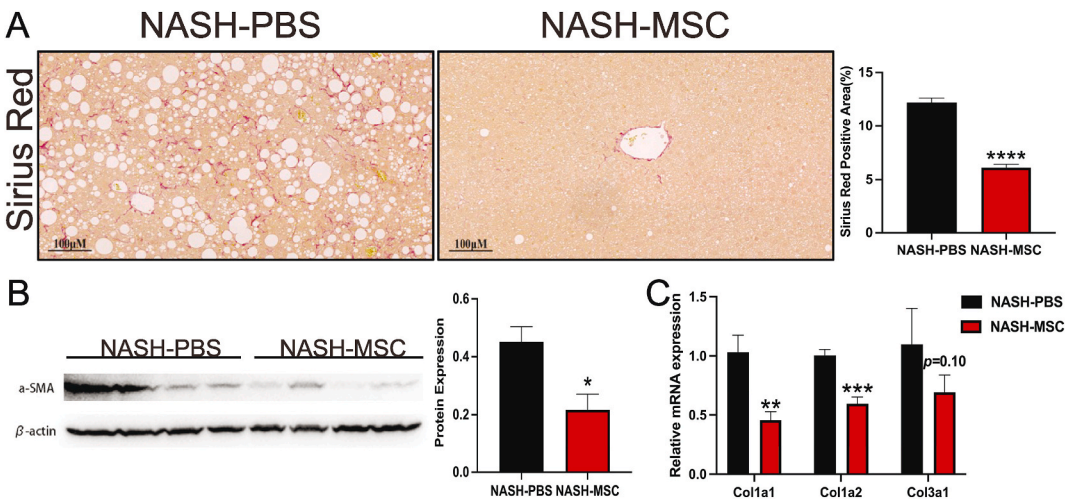

Fig. 4. hUC-MSCs treatment significantly attenuated NASH-related fibrosis in mice (A) Sirius Red staining (left) and positive area quantification (right) of liver sections from two groups of mice (n = 4–5 mice/group). The positive area was quantified by Image J. Scale bars, 100 μm. (B) α-SMA protein expression in livers of indicated groups. (n = 4 mice/group). (the uncropped versions of the figures can be found in the supplement file). (C) Relative mRNA levels of fibrosis-related genes in livers of indicated groups (n = 4 mice/group).

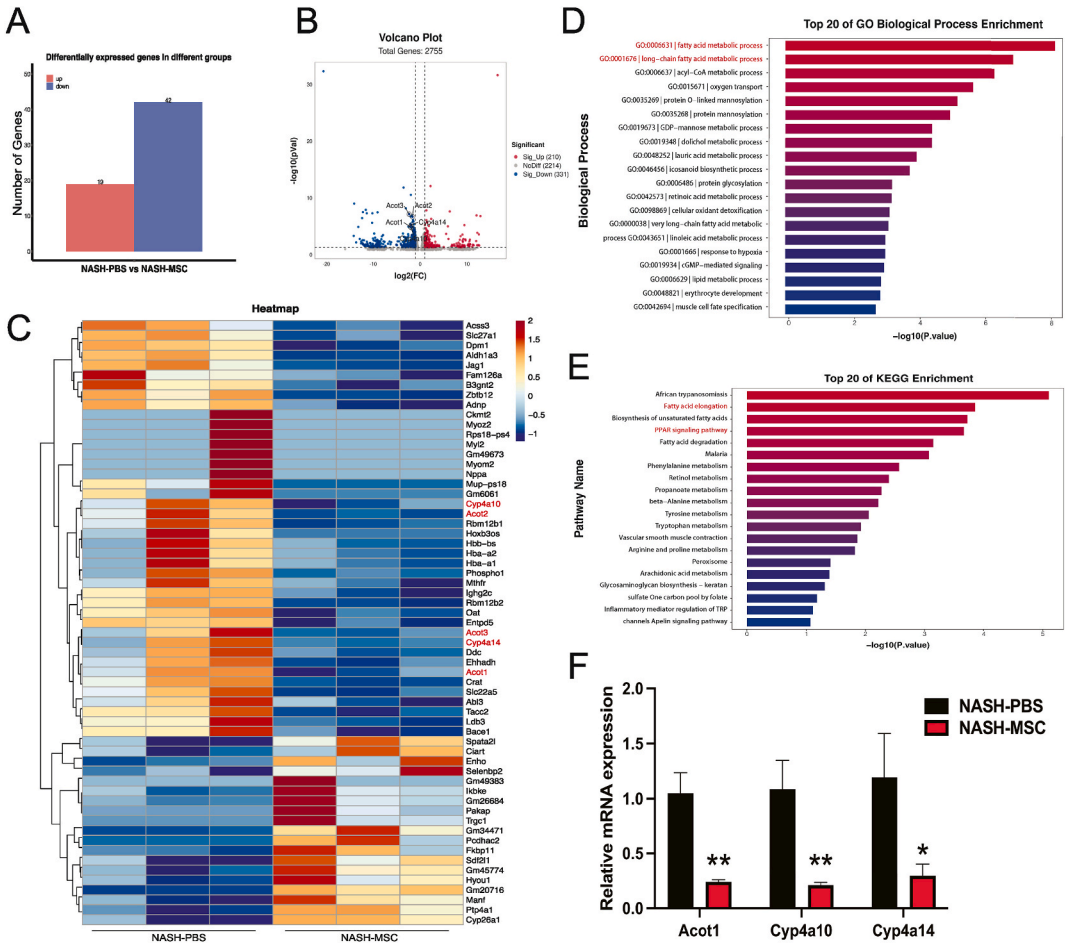

Fig. 5. hUC-MSCs administration relieved NASH by inhibiting the ACOT Gene Cluster and Cyp4a Family Members (Cyp4a10/Cyp4a14) (A) Barplot of differentially expressed genes between the two groups ($n = 3$). (B) Volcano plot showing significantly altered genes. The tagged genes represent our metabolites of interest. (C) The heatmap showing the differential abundance of genes in MSC-treated mice (NASH-MSC) versus PBS-treated (NASH-PBS). Red labels indicated metabolites that were selected decreased in MSC-treated mice. $P < 0.05$, $|\text{Log2FC}| > 1$. (D) KEGG pathway enrichment analysis on DEGs. Fatty acid elongation and PPAR signaling pathway are highlighted. (E) GO biological process enrichment analysis on DEGs. Fatty acid metabolic processes and long-chain are highlighted. (F) Validation of some differentially expressed genes by qPCR in mouse livers. Biological repetition ($n = 4$).

Several other studies have demonstrated that *Acot1*, *Acot2*, *Acot3*, *Cyp4a10*, and *Cyp4a14* are closely related to steatosis, inflammation, and liver fibrosis [23–28]. Thus, *Acot1*, *Cyp4a10*, and *Cyp4a14* were selected for further validation by qPCR in the livers of both groups, with the expression of all three genes decreasing significantly in the hUC-MSC-treated group (Fig. 5F). The application of hUC-MSCs mitigated NASH by downregulating Acot1 in fatty acid metabolism and reducing the expression of Cyp4a10 and Cyp4a14 in the PPAR signaling pathway.

4. Discussion

The prevalence of obesity and diabetes has increased worldwide, resulting in a consequent increase in the incidence of NASH. NASH represents the most critical step in the progression of chronic liver disease to end-stage liver disease; nonetheless, no anti-NASH or anti-fibrosis drugs are currently available on the market. Most drugs currently investigated by clinical trials predominantly target four main pathways. The first strategy aims to reduce hepatic fat deposition, and medications that employ this strategy regulate PPAR signaling. The second strategy targets oxidative stress, inflammation, and apoptosis. The third strategy involves warding off intestinal microbiomes and metabolic endotoxemia. The final strategy aims to prevent hepatic fibrosis, which is closely linked to all-cause or liver-related mortality in NASH [8]. Among these, the most likely successful drugs mainly reduce liver fat accumulation and anti-fibrosis. However, no drug can target these multiple therapeutic targets.

MSCs are non-hematopoietic cells that can be reliably isolated from bone marrow, adipose tissues, fetal tissues, and umbilical cords [29]. MSCs can migrate into wounded areas, differentiate into local components, and release chemokines, cytokines, and growth

factors that aid tissue repair [30]. MSCs also possess unique immunophenotypic and immunoregulatory properties. Treating chronic liver disease using MSCs has recently become a hot topic in stem cell research. hUC-MSCs have been shown to migrate to injured liver tissues to promote liver regeneration [31]. MSCs have been reported to suppress fibrogenesis and inflammation in a chronic liver injury model [32]. Human BM-MSCs are known to alleviate high-fat diet (HFD)-induced NASH in mouse livers by reducing hepatic lipid accumulation and inflammation [33]. Moreover, researchers believe that BM-MSCs may have an immunomodulatory function in the treatment of liver fibrosis by inhibiting interleukin-17A (IL17A), which has an impact on the interleukin-6 (IL6)/signal transducer and activator of transcription 3 (STAT3) signaling pathway [34]. Concerning their immune-modulating function, BM-MSCs treated with heme oxygenase 1 (HO-1) improve poor liver transplant survival by reducing inflammatory responses and acute cellular rejection [35]. Human adipose-derived MSCs have also been reported to alleviate hepatic ischemia-reperfusion injury and improve liver repair [36]. Over the past decades, few studies have demonstrated that MSCs can ameliorate NAFLD/NASH. Mouse BM-MSC administration can prevent the deterioration of HFD-induced NAFLD [37]. Mouse UC-MSC exosomes have been reported to exert a protective effect on methionine-choline-deficient (MCD) diet-induced NASH in mice [38]. An artificial MCD diet rapidly induces steatosis, fibrosis, and an inflammatory liver phenotype. Nevertheless, systemic NASH symptoms linked to insulin resistance, including metabolic syndrome, are absent. Thus, MSCs provide a novel option for multi-target therapies for NASH. HUC-MSCs are produced from umbilical cords and possess multiple advantages over other types of stem cells, such as no tumorigenicity, karyotype stability, high immunomodulation, minimal risk of graft-versus-host disease, minimal chance of transmitting somatic mutations or infectious diseases, and low immunogenicity [39].

Furthermore, their collection does not require an invasive method and does not cause the same ethical concerns associated with using human embryonic stem cells. WD contains high fat, cholesterol, and fructose, which can induce NASH in mice, like human diseases [40,41]. Therefore, based on the above merits, hUC-MSCs were used as a treatment in the WD-induced NASH model in our study.

Steatosis, insulin resistance, inflammation, and fibrosis are the key steps in the progression of NASH. Insulin resistance leads to lipid accumulation in hepatocytes. It increases their sensitivity to internal and exogenous damaging factors, leading to lipid peroxidation and related events caused by reactive oxygen species, which leads to steatohepatitis. Steatohepatitis persists, extracellular matrix synthesis exceeds degradation, and progressive liver fibrosis occurs. High-throughput genomic research, such as microarrays, array-based comparative genomic hybridization, and deep sequencing, combined with bioinformatics and other computational biology approaches [42], have recently identified numerous genes deregulated during NAFLD and NASH development. In our study, NASH remission was found to be closely related to the expression of several genes involved in fatty acid metabolic processes, including *Acot1*, *Acot2*, and *Acot3*. In addition, *Cyp4a10* and *Cyp4a14*, which are related to the PPAR signaling pathway, were also downregulated. The ACOT family is important in lipid metabolism as it regulates the quantities and ratios of activated and free fatty acids. The mouse ACOT gene cluster consists of six genes: *Acot1* in the cytosol, *Acot2* in the mitochondria, and *Acot3–6* in peroxisomes [43]. *Acot1* is predominantly expressed in the liver, kidneys, and hearts of mice. Franklin et al. [24] found that Acot1 knockout increased fatty acid oxidation and significantly decreased liver triglyceride (TG) content. Overexpression of *Acot2* in the liver leads to increased oxidation of fatty acids in vivo. Recently, some researchers have predicted that an increase in *Acot2* expression may be an important feature of abnormal lipid metabolism [25]. Another study indicated that high fructose corn syrup consumption significantly increases *Acot2* and *Acot3* expression in mice [26]. In the liver, murine *Cyp4a10* and *Cyp4a14* (homologous to human *CYP4A22* and *CYP4A11*, respectively) were found to be substantially expressed. Yang et al. [27] reported that *Cyp4a10* and *Cyp4a14* overexpression promoted lipid accumulation and oxidative stress. Zhang et al. [28] showed that inhibition of *Cyp4a14* could improve HFD-induced hepatic steatosis and MCD-induced steatohepatitis, liver injury, and liver fibrosis. *Cyp4a10* and *Cyp4a14* may be involved in the microsomal oxidation of medium-to-long-chain fatty acids [28] and alternative catalysts for microsomal oxidative stress to induce NASH [44]. Among these, important evidence from existing literature [23] showed that *Acot1* knockout also decreased the expression of *PPARα* target genes, such as *Cyp4a10* and *Cyp4a14*. Therefore, in this study, we hypothesized that hUC-MSCs downregulate *Cyp4a10* and *Cyp4a1*4 by downregulating *Acot1*; however, this theory requires further experimental verification.

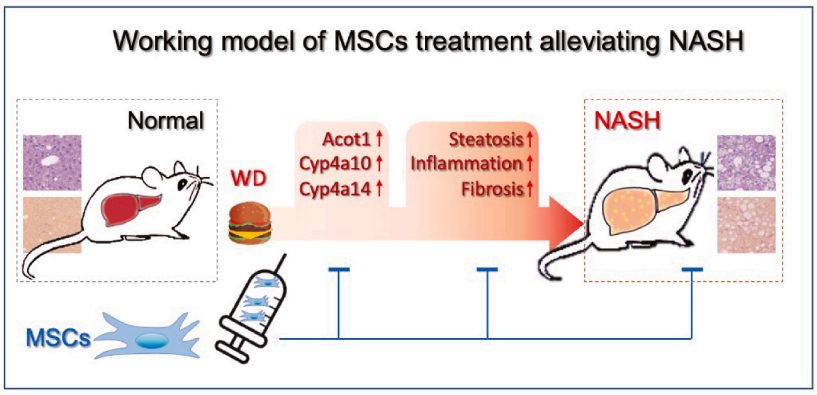

Fig. 6. hUC-MSCs serve as an efficient treatment for WD-induced obesity, NASH, and fibrosis.

In recent years, a new technology, in vivo imaging, can dynamically observe the migration process of MSCs after entering the mouse body, and clarify whether MSCs reach the tissues in need of repair as expected [46,47]. However, in vivo imaging technique was not used in our study based on the following considerations: First, Numerous studies, including in vivo imaging tracer techniques, have demonstrated that MSCs would migrate through the vascular endothelium to the site of injury when the experimental animals are in a pathological condition, which is called the "homing effect" [48]. Second, Our study showed that the livers of mice had a typical phenotype of NASH, a chronic inflammatory state, so we speculated that hUC-MSCs would act on the liver through its "homing" to the site of inflammation. Actually, it was confirmed liver steatosis and inflammation were greatly improved after hUC-MSCs transplatation; Finally, current research suggests that stem cells have therapeutic effects primarily through the paracrine mechanism [49]. However, in vivo imaging is a terrific way to visualize tracing MSCs, and we will try to use this technique in future work, which will help us to better explore the mechanism of hUC-MSCs therapy for NASH.

This study uncovered several critical functions of hUC-MSCs in improving WD-induced obesity and NASH. First, hUC-MSC therapy improved insulin sensitivity, consistent with prior results [45]. Second, at least partially, hUC-MSCs downregulated genes related to lipid metabolism, inflammation, and fibrosis expression by decreasing fatty acid metabolic progress and PPAR signaling pathway gene expression (particularly *Acot1*, *Cyp4a10*, and *Cyp4a14*). Although our study confirmed that hUC-MSCs serve as an efficient treatment for WD-induced obesity, NASH, and fibrosis (a hypothetical mechanism diagram is shown in Fig. 6), the underlying mechanism needs to be further explored. In the future, the application prospect of stem cells in other liver diseases, such as autoimmune liver diseases and drug-induced liver injury, ischemia-reperfusion injury, and so on, will be expanded by utilizing its multi-directional differentiation potential, tissue repair function, and immunomodulatory ability.

5. Conclusion

In summary, the present study showed for the first time that hUC-MSC transplantation had a positive effect on WD-induced obesity, NASH, and fibrosis, which acted, at least in part, through the regulation of key genes involved in glucose and lipid metabolism. Further studies are required to evaluate the exact mechanisms underlying this effect.

Consent for publication

No applicable.

Funding

This research was funded by the General Program of the National Natural Science Foundation of China (Grant No. 82270639), the Scientific research project of the Shanghai Municipal Health Committee (Grant No. 202240001), the Specialty Feature Construction Project of Shanghai Pudong New Area Health Commission (Grant No. PWZzb2022-05), Technology Development Project of Pudong Science, Technology and Economic Commission of Shanghai (Grant No. PKJ2021-Y08), the Natural Science Foundation of the Xinjiang Uygur Autonomous Region (Grant No. 2022D01A24), Key Disciplines Group Construction Project of Shanghai Pudong New Area Health Commission (Grant No.PWZxq2022-06), Medical discipline Construction Project of Pudong Health Committee of Shanghai (Grant No.PWYgf2021-02) and Peak Disciplines (Type IV) of Institutions of Higher Learning in Shanghai.

CRediT authorship contribution statement

Jiali Hu: Writing – original draft, Visualization, Software, Methodology, Investigation, Formal analysis, Conceptualization. **Shan Li:** Writing – review & editing, Validation, Methodology, Formal analysis, Data curation, Conceptualization. **Xuan Zhong:** Writing – original draft, Validation. **Yushuang Wei:** Resources. **Qinjuan Sun:** Formal analysis. **Lan Zhong:** Writing – review & editing, Supervision, Project administration, Funding acquisition.

Declaration of competing interest

Jiali Hu, Shan Li, Lan Zhong has patent pending to Jiali Hu, Shan Li, Lan Zhong. The authors declare that they have no other known competing financial interests or personal relationships that could have appeared to influence the work reported in this paper.

Acknowledgments

The authors thank Guangxi Zhao, Changsheng Du, and Zihui Tang for their excellent technical assistance.

Appendix A. Supplementary data

Supplementary data to this article can be found online at https://doi.org/10.1016/j.heliyon.2024.e25460.

References

[1] J.V. Lazarus, H.E. Mark, Q.M. Anstee, J.P. Arab, R.L. Batterham, L. Castera, H. Cortez-Pinto, J. Crespo, K. Cusi, M.A. Dirac, et al., Advancing the global public health agenda for NAFLD: a consensus statement, Nat. Rev. Gastroenterol. Hepatol. 19 (1) (2022 Jan) 60–78, https://doi.org/10.1038/s41575-021-00523-4. Epub 2021 Oct 27. PMID: 34707258.

[2] F. Piscaglia, G. Svegliati-Baroni, A. Barchetti, A. Pecorelli, S. Marinelli, C. Tiribelli, S. Bellentani, HCC-NAFLD Italian Study Group. Clinical patterns of hepatocellular carcinoma in non-alcoholic fatty liver disease: a multicenter prospective study, Hepatology 63 (2016) 827–838, https://doi.org/10.1002/hep.28368.

[3] E.E. Powell, V.W. Wong, M. Rinella, Non-alcoholic fatty liver disease, Lancet 397 (2021) 2212–2224, https://doi.org/10.1016/S0140-6736(20)32511-3.

[4] T.C. Yip, H.W. Lee, W.K. Chan, G.L. Wong, V.W. Wong, Asian perspective on NAFLD-associated HCC, J. Hepatol. 76 (2022) 726–734, https://doi.org/10.1016/j.jhep.2021.09.024.

[5] Z.M. Younossi, A.B. Koenig, D. Abdelatif, Y. Fazel, L. Henry, M. Wymer, Global epidemiology of non-alcoholic fatty liver disease-Meta-analytic assessment of prevalence, incidence, and outcomes, Hepatology 64 (2016) 73–84, https://doi.org/10.1002/hep.28431.

[6] C.R. Wong, J.K. Lim, The association between non-alcoholic fatty liver disease and cardiovascular disease outcomes, Clin. Liver Dis. 12 (2018) 39–44, https://doi.org/10.1002/cld.721.

[7] D. Schuppan, R. Surabattula, X.Y. Wang, Determinants of fibrosis progression and regression in NASH, J. Hepatol. 68 (2018) 238–250, https://doi.org/10.1016/j.jhep.2017.11.012.

[8] Y. Sumida, M. Yoneda, Current and future pharmacological therapies for NAFLD/NASH, J. Gastroenterol. 53 (2018) 362–376, https://doi.org/10.1007/s00535-017-1415-1.

[9] M. Krampera, Mesenchymal stromal cell 'licensing': a multistep process, Leukemia 25 (2011) 1408–1414, https://doi.org/10.1038/leu.2011.108.

[10] C. Toma, A. Fisher, J. Wang, X. Chen, M. Grata, J. Leeman, B. Winston, M. Kaya, H. Fu, L. Lavery, et al., Vascular endoluminal delivery of mesenchymal stem cells using acoustic radiation force, Tissue Eng. 17 (2011) 1457–1464, https://doi.org/10.1089/ten.TEA.2010.0539.

[11] K. Le Blanc, F. Frassoni, L. Ball, F. Locatelli, H. Roelofs, I. Lewis, E. Lanino, B. Sundberg, M.E. Bernardo, M. Remberger, et al., Developmental Committee of the European Group for Blood and Marrow Transplantation. Mesenchymal stem cells for treatment of steroid-resistant, severe, acute graft-versus-host disease: a phase II study, Lancet 371 (9624) (2008) 1579–1586, https://doi.org/10.1016/S0140-6736(08)60690-X. PMID: 18468541.

[12] J. Galipeau, L. Sensébé, Mesenchymal stromal cells: clinical challenges and therapeutic opportunities, Cell Stem Cell 22 (2018) 824–833, https://doi.org/10.1016/j.stem.2018.05.004.

[13] F. de la Portilla, F. Alba, D. García-Olmo, J.M. Herrerías, F.X. González, A. Galindo, Expanded allogeneic adipose-derived stem cells (eASCs) for the treatment of complex perianal fistula in Crohn's disease: results from a multicenter phase I/IIa clinical trial, Int. J. Colorectal Dis. 28 (2013) 313–323, https://doi.org/10.1007/s00384-012-1581-9.

[14] G. Moll, J.A. Ankrum, J. Kamhieh-Milz, K. Bieback, O. Ringdén, H.D. Volk, S. Geissler, P. Reinke, Intravascular mesenchymal stromal/stem cell therapy product diversification: time for new clinical guidelines, Trends Mol. Med. 25 (2) (2019) 149–163, https://doi.org/10.1016/j.molmed.2018.12.006. Epub 2019 Jan 30. PMID: 30711482.

[15] W. Luo, Y. Gong, F. Qiu, Y. Yuan, W. Jia, Z. Liu, L. Gao, NGF nanoparticles enhance the potency of transplanted human umbilical cord mesenchymal stem cells for myocardial repair, Am. J. Physiol. Heart Circ. Physiol. 320 (2021) H1959–H1974, https://doi.org/10.1152/ajpheart.00855.2020.

[16] A. Kechin, U. Boyarskikh, A. Kel, M. Filipenko, cutPrimers: a new tool for accurate cutting of primers from reads of targeted next generation sequencing, J. Comput. Biol. 24 (2017) 1138–1143, https://doi.org/10.1089/cmb.2017.0096.

[17] D. Kim, J.M. Paggi, C. Park, C. Bennett, S.L. Salzberg, Graph-based genome alignment and genotyping with HISAT2 and HISAT-genotype, Nat. Biotechnol. 37 (2019) 907–915, https://doi.org/10.1038/s41587-019-0201-4.

[18] S. Kovaka, A.V. Zimin, G.M. Pertea, R. Razaghi, S.L. Salzberg, M. Pertea, Transcriptome assembly from long-read RNA-seq alignments with StringTie2, Genome Biol. 20 (2019) 278, https://doi.org/10.1186/s13059-019-1910-1.

[19] G. Pertea, M. Pertea, GFF Utilities: GffRead and GffCompare. F1000Res, 2020, p. 9, https://doi.org/10.12688/f1000research.23297.2.

[20] M. Pertea, D. Kim, G.M. Pertea, J.T. Leek, S.L. Salzberg, Transcript-level expression analysis of RNA-seq experiments with HISAT, StringTie and Ballgown, Nat. Protoc. 11 (2016) 1650–1667, https://doi.org/10.1038/nprot.2016.095.

[21] M. Dominici, K. Le Blanc, I. Mueller, I. Slaper-Cortenbach, F. Marini, D. Krause, R. Deans, A. Keating, Dj Prockop, E. Horwitz, Minimal criteria for defining multipotent mesenchymal stromal cells. The International Society for Cellular Therapy position statement, Cytotherapy 8 (4) (2006) 315–317, https://doi.org/10.1080/14653240600855905. PMID: 16923606.

[22] P. Bourin, B.A. Bunnell, L. Casteilla, M. Dominici, A.J. Katz, K.L. March, H. Redl, J.P. Rubin, K. Yoshimura, J.M. Gimble, Stromal cells from the adipose tissue-derived stromal vascular fraction and culture expanded adipose tissue-derived stromal/stem cells: a joint statement of the International Federation for Adipose Therapeutics and Science (IFATS) and the International Society for Cellular Therapy (ISCT), Cytotherapy 15 (6) (2013) 641–648, https://doi.org/10.1016/j.jcyt.2013.02.006. Epub 2013 Apr 6. PMID: 23570660; PMCID: PMC3979435.

[23] M.P. Franklin, A. Sathyanarayan, D.G. Mashek, Acyl-CoA thioesterase 1 (ACOT1) regulates PPARα to couple fatty acid flux with oxidative capacity during fasting, Diabetes 66 (2017) 2112–2123, https://doi.org/10.2337/db16-1519.

[24] C. Moffat, L. Bhatia, T. Nguyen, P. Lynch, M. Wang, D. Wang, O.R. Ilkayeva, X. Han, M.D. Hirschey, S.M. Claypool, et al., Acyl-CoA thioesterase-2 facilitates mitochondrial fatty acid oxidation in the liver, J. Lipid Res. 55 (12) (2014) 2458–2470, https://doi.org/10.1194/jlr.M046961. Epub 2014 Aug 11. PMID: 25114170; PMCID: PMC4242439.

[25] X. Yin, C. Lyu, Z. Li, Q. Wang, Y. Ding, Y. Wang, Y. Qiu, S. Cui, D. Guo, R. Xu, High expression of ACOT2 predicts worse overall survival and abnormal lipid metabolism: a potential target for acute myeloid leukemia, J Healthc Eng 2022 (2022) (2022) 2669114, https://doi.org/10.1155/2022/2669114. PMID: 36193167; PMCID: PMC9525752.

[26] Y. Shen, Y. Sun, X. Wang, Y. Xiao, L. Ma, W. Lyu, Z. Zheng, W. Wang, J. Li, Liver transcriptome and gut microbiome analysis reveals the effects of high fructose corn syrup in mice, Front. Nutr. 9 (2022) 921758, https://doi.org/10.3389/fnut.2022.921758. PMID: 35845805; PMCID: PMC9280673.

[27] Z. Yang, R.V. Smalling, Y. Huang, Y. Jiang, P. Kusumanchi, W. Bogaert, L. Wang, D.A. Delker, N.J. Skill, S. Han, et al., The role of SHP/REV-ERBα/CYP4A axis in the pathogenesis of alcohol-associated liver disease, JCI Insight (2021) 6, https://doi.org/10.1172/jci.insight.140687.

[28] X. Zhang, S. Li, Y. Zhou, W. Su, X. Ruan, B. Wang, F. Zheng, M. Warner, J.Å. Gustafsson, Y. Guan, Ablation of cytochrome P450 omega-hydroxylase 4A14 gene attenuates hepatic steatosis and fibrosis, Proc. Natl. Acad. Sci. U.S.A. 114 (2017) 3181–3185, https://doi.org/10.1073/pnas.1700172114.

[29] W. Lin, L. Huang, Y. Li, B. Fang, G. Li, L. Chen, L. Xu, Mesenchymal stem cells and cancer: clinical challenges and opportunities, BioMed Res. Int. 2019 (2019) 2820853, https://doi.org/10.1155/2019/2820853.

[30] X. Fu, G. Liu, A. Halim, Y. Ju, Q. Luo, Song AG Mesenchymal stem cell migration and tissue repair, Cells (2019) 8, https://doi.org/10.3390/cells8080784.

[31] Kim D.H., Je CM, Sin J.Y., Jung J.S. (20003) Effect of partial hepatectomy on in vivo engraftment after intravenous administration of human adipose tissue stromal cells in mouse. Microsurgery. 23, 424-431 [doi:10.1002/micr.10178].

[32] B. Huang, X. Cheng, H. Wang, W. Huang, Z. la Ga hu, D. Wang, K. Zhang, H. Zhang, Z. Xue, Y. Da, et al., Mesenchymal stem cells and their secreted molecules predominantly ameliorate fulminant hepatic failure and chronic liver fibrosis in mice respectively, J. Transl. Med. 14 (2016) 45, https://doi.org/10.1186/s12967-016-0792-1.

[33] S. Nickel, M. Christ, S. Schmidt, J. Kosacka, H. Kühne, M. Roderfeld, T. Longerich, L. Tietze, I. Bosse, M.J. Hsu, et al., Human mesenchymal stromal cells resolve lipid load in high fat diet-induced non-alcoholic steatohepatitis in mice by mitochondria donation, Cells (2022) 11, https://doi.org/10.3390/cells11111829.

[34] S. Farouk, S. Sabet, F.A. Abu Zahra, A.A. El-Ghor, Bone marrow derived-mesenchymal stem cells downregulate IL17A dependent IL6/STAT3 signaling pathway in CCl4-induced rat liver fibrosis, PLoS One 13 (2018) e0206130, https://doi.org/10.1371/journal.pone.0206130.

[35] B. Wu, H. Song, Y. Yang, M. Yin, B. Zhang, Y. Cao, C. Dong, Z. Shen, Improvement of liver transplantation outcome by heme Oxygenase-1-Transduced bone marrow mesenchymal stem cells in rats, Stem Cell. Int. 2016 (2016) 9235073, https://doi.org/10.1155/2016/9235073.

[36] R.F. Saidi, B. Rajeshkumar, A. Shariftabrizi, A.A. Bogdanov, S. Zheng, K. Dresser, et al., Human adipose-derived mesenchymal stem cells attenuate liver ischemia-reperfusion injury and promote liver regeneration, Surgery 156 (2014) 1225–1231, https://doi.org/10.1016/j.surg.2014.05.008.
[37] M. Ezquer, F. Ezquer, M. Ricca, C. Allers, P. Conget, Intravenous administration of multipotent stromal cells prevents the onset of non-alcoholic steatohepatitis in obese mice with metabolic syndrome, J. Hepatol. 55 (2011) 1112–1120, https://doi.org/10.1016/j.jhep.2011.02.020.
[38] Y. Shi, X. Yang, S. Wang, Y. Wu, L. Zheng, Y. Tang, Y. Gao, J. Niu, Human umbilical cord mesenchymal stromal cell-derived exosomes protect against MCD-induced NASH in a mouse model, Stem Cell Res. Ther. 13 (2022) 517, https://doi.org/10.1186/s13287-022-03201-7.
[39] I. Anwar, U.A. Ashfaq, Z. Shokat, Therapeutic potential of umbilical cord stem cells for liver regeneration, Curr. Stem Cell Res. Ther. 15 (2020) 219–232, https://doi.org/10.2174/1568026620666200220122536.
[40] D. Soleimani, G. Ranjbar, R. Rezvani, L. Goshayeshi, F. Razmpour, M. Nematy, Dietary patterns in relation to hepatic fibrosis among patients with non-alcoholic fatty liver disease, Diabetes Metab Syndr Obes 12 (2019) 315–324, https://doi.org/10.2147/DMSO.S198744.
[41] K. Stephenson, L. Kennedy, L. Hargrove, J. Demieville, J. Thomson, G. Alpini, H. Francis, Updates on dietary models of non-alcoholic fatty liver disease: current studies and insights, Gene Expr. 18 (2018) 5–17, https://doi.org/10.3727/105221617X15093707969658.
[42] C.W. Wernberg, K. Ravnskjaer, M.M. Lauridsen, M. Thiele, The role of diagnostic biomarkers, omics strategies, and single-cell sequencing for non-alcoholic fatty liver disease in severely obese patients, J. Clin. Med. 10 (2021), https://doi.org/10.3390/jcm10050930.
[43] M.C. Hunt, A. Rautanen, M.A. Westin, L.T. Svensson, S.E. Alexson, Analysis of the mouse and human acyl-CoA thioesterase (ACOT) gene clusters shows that convergent, functional evolution results in a reduced number of human peroxisomal ACOTs, Faseb. J. 20 (2006) 1855–1864, https://doi.org/10.1096/fj.06-6042com.
[44] I.A. Leclercq, G.C. Farrell, J. Field, D.R. Bell, F.J. Gonzalez, G.R. Robertson, CYP2E1 and CYP4A as microsomal catalysts of lipid peroxides in murine non-alcoholic steatohepatitis, J. Clin. Invest. 105 (2000) 1067–1075, https://doi.org/10.1172/JCI8814.
[45] Y. Sun, H. Shi, S. Yin, C. Ji, X. Zhang, B. Zhang, P. Wu, Y. Shi, F. Mao, Y. Yan, et al., Human mesenchymal stem cell derived exosomes alleviate type 2 diabetes mellitus by reversing peripheral insulin resistance and relieving β-cell destruction, ACS Nano 12 (2018) 7613–7628, https://doi.org/10.1021/acsnano.7b07643.
[46] S. Chen, Z. Lu, H. Jia, B. Yang, C. Liu, Y. Yang, S. Zhang, Z. Wang, L. Yang, S. Li, J. Li, C. Yang, Hepatocyte-specific Mas activation enhances lipophagy and fatty acid oxidation to protect against acetaminophen-induced hepatotoxicity in mice, J. Hepatol. 78 (3) (2023) 543–557, https://doi.org/10.1016/j.jhep.2022.10.028.
[47] Z. Lu, Y. Liu, M. Jin, X. Luo, H. Yue, Z. Wang, S. Zuo, Y. Zeng, J. Fan, Y. Pang, J. Wu, J. Yang, Q. Dai, Virtual-scanning light-field microscopy for robust snapshot high-resolution volumetric imaging, Nat. Methods 20 (5) (2023) 735–746, https://doi.org/10.1038/s41592-023-01839-6.
[48] M. Krampera, K. Le Blanc, Mesenchymal stromal cells: putative microenvironmental modulators become cell therapy, Cell Stem Cell 28 (10) (2021) 1708–1725, https://doi.org/10.1016/j.stem.2021.09.006.
[49] M. Gnecchi, P. Danieli, G. Malpasso, M.C. Ciuffreda, Paracrine mechanisms of mesenchymal stem cells in tissue repair, Methods Mol. Biol. 1416 (2016) 123–146, https://doi.org/10.1007/978-1-4939-3584-0_7.